

Detection of Vesicoureteral Reflux using Electrical Impedance Tomography

Eoghan Dunne, *Student Member, IEEE*, Martin O'Halloran, *Member, IEEE*, Darren Craven, Prem Puri, Paul Frehill, Sarah Loughney, Emily Porter, *Member, IEEE*

Abstract— Objective: The purpose of this study is to detect vesicoureteral reflux (VUR) non-invasively using electrical impedance tomography (EIT). VUR is characterized by the backflow of urine from the bladder to the kidneys. **Methods:** Using porcine models, small quantities of a solution mimicking the electrical properties of urine were infused into each ureter. EIT measurements were taken before, during and after the infusion using electrodes positioned around the abdomen. The collected data from 116 experiments were then processed and time-difference images reconstructed. Objective VUR detection was determined through statistical analysis of the mean change in the voltage signals and EIT image pixel intensities. **Results:** Unilateral VUR was successfully detected in 94.83% of all mean voltage signals and in over 98.28% of the reconstructed images. The images showed strong visual contrast between the region of interest and the background. **Conclusion:** In animal models, EIT has the capability to detect reflux in the kidneys with high accuracy. The results show promise for EIT to be used for screening of VUR in children. **Significance:** VUR is the most common congenital urinary tract abnormality in children. The condition predisposes children to urinary tract infections (UTIs) and kidney damage. The current gold standard diagnostic test, a voiding cystourethrogram (VCUG), is invasive and uses ionizing radiation; therefore, there is a need for new tools for identifying VUR in children. This study presents a non-invasive method to detect VUR in animal models, illustrating the potential for EIT as a screening tool in clinical scenarios.

Index Terms— Electrical Impedance Tomography, Vesicoureteral Reflux (VUR), Animal Study

I. INTRODUCTION

PRIMARY vesicoureteral reflux (VUR), the retrograde flow of urine from the bladder to the kidneys, is the most

This project was funded by Enterprise Ireland and the European Regional Development Fund (ERDF) under Ireland's European Structural and Investment Funds Programme 2014-2020. The research was also supported by the European Research Council under the European Union's Horizon 2020 Programme/ERC Grant Agreement BioElecPro n. 637780 and the charity RESPECT and the People Programme (Marie Curie Actions) of the European Union's Seventh Framework Programme (FP7/2007-2013) under REA Grant Agreement no. PCOFUND-GA-2013-608728.

E. Dunne and E. Porter are with the Translational Medical Device Lab (TMD Lab) and the Department of Electrical & Electronic Engineering at the NUI Galway, Ireland (corresponding email: e.dunne13@nuigalway.ie).

M. O'Halloran is the Director of the TMD Lab and is with the Department of Electrical & Electronic Engineering and the Department of Medicine at the National University of Ireland Galway.

D. Craven, P. Puri, P. Frehill and S. Loughney are with the company Kite Medical (kitemedical.ie). Kite Medical, with the assistance of Enterprise Ireland, provided funding to the TMD Lab in respect of this research.

common urological anomaly in children. With a prevalence of 2-3% in the pediatric population, the condition occurs in 30-40% of children who present with Urinary Tract Infections (UTIs) [1], [2]. The hereditary and familial nature of VUR is now well recognized and several studies have shown that siblings of children with VUR have a much higher incidence of reflux than the general pediatric population. Prevalence rates of 27-51% in siblings of children with VUR and 66% rate of VUR in offspring of parents with previously diagnosed reflux have been reported [3].

There are five grades of VUR as defined by the International Reflux Study Committee [4]. Each grade is based on the severity of backflow of urine and degree of dilation of the ureters and kidneys, as shown in Fig. 1. Moderate to severe cases (Grade III VUR or higher) of VUR account for approximately 27% of all patients diagnosed with VUR [5].

Methods that are most widely used to detect VUR in clinical practice include voiding cystourethrogram (VCUG) and, more recently, Voiding Urosonography (VUS). The VCUG procedure involves radiation exposure and both procedures require catheterization and observed voiding to allow the physician to capture images or take measurements. VCUG is the gold standard based on the precise anatomic details provided that allows accurate grading of VUR. Guidelines also recommend that ultrasound is performed on any infant with suspicion of VUR to detect anatomical abnormalities in the ureters or kidneys. However, ultrasound is not sufficiently sensitive for detecting VUR (the estimated average sensitivity of ultrasound is 0.44 with a 95% confidence interval of 0.34 to 0.54 [6]).

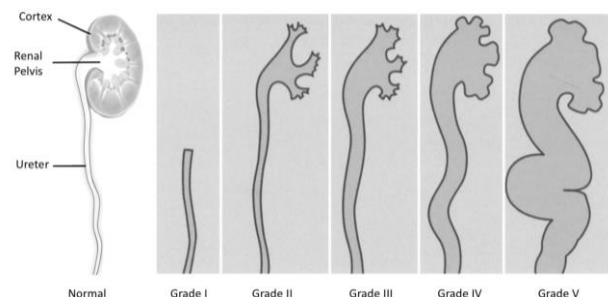


Fig. 1. Illustration showing normal (healthy) upper urinary tract and the international classification of VUR (grades I-V). As the grades increase, there is more backflow of urine to the kidney. The ureter becomes more dilated and tortuous and the collecting system in the kidney also dilates.

The challenges associated with the VUCG examination include bladder catheterization, injection of contrast agent and x-ray imaging. Urethral catheterization is not well tolerated by children and sedation is occasionally required, incurring additional costs, time and stress to parents and children. Radiation exposure is also a significant disadvantage. Additionally, there is significant inter-observer variability that is associated with VUCG readings and hence grading and diagnostic outcome [7], [8], [9].

The consequences of missed diagnosis of higher grade VUR (III-V) can be severe, potentially leading to renal scarring or renal parenchymal damage. Acquired scarring results from pyelonephritis induced renal injury, whereas congenital reflux nephropathy is a result of abnormal embryological development with subsequent renal dysplasia. Exposure to UTIs in patients with congenital renal dysplasia can lead to progression of renal parenchymal damage. VUR associated nephropathy is an important cause of hypertension and end-stage renal disease (ESRD) [10], [11]. The UK Renal Registry Report revealed that renal dysplasia/VUR remained the most common cause of ESRD in children under 16 years of age (32%) [12].

Electrical impedance tomography (EIT) is a safe, low-cost and portable medical imaging technology. To date, EIT has been primarily investigated in clinical settings to monitor patients under mechanical ventilation [13]. EIT involves injecting small alternating currents into the tissue and measuring the resultant voltages in order to construct a conductivity-based image of the region. The resultant voltages or images may be then used by clinicians to diagnose or monitor a certain clinical condition. EIT is particularly suitable where bodily mechanisms change with time due to the technology having a strong temporal resolution. For example, applications involving monitoring of breathing and of urine volume [13], [14]. EIT-based devices can also provide real-time feedback to clinicians. Thus, EIT offers a promising solution for the screening of VUR.

In this study, we perform the first investigation (to our knowledge) of the use of EIT to detect VUR. We test the ability of an EIT system in detecting unilateral VUR at the kidney of animal models with low volumes of backflow. We perform a large number of experiments (> 100) and objectively evaluated detection based on raw voltage data and images using statistical analysis.

This paper is structured as follows: Section II describes the methodology of the study; Section III outlines the data processing; Section IV details the objective detection of backflow into the kidneys; Section V presents the results; Section VI concludes the paper.

II. METHODS

In this section, we discuss the animal models, the experimental setup, and the measurement procedure.

A. Ethical Approval

The animal study was ethically approved by the Animal Experiments Inspectorate for the Ministry of Environment and

Food of Denmark (reference number: 2015-15-0201-00476) and the procedure was completed in the Department of Clinical Medicine at Aarhus University, Denmark. The study was conducted in line with all local and national guidelines.

B. EIT Hardware

In this study, we used the commercially-available Swisstom Pioneer EIT device (Swisstom AG, Landquart, Switzerland) with 32 fabric electrodes arranged in a belt configuration. The device and belt are shown in Fig. 2.

The fabric belt was custom made and consisted of 10 cm long cables soldered directly to the Swisstom Pioneer belt. A stud ring terminal was connected to the opposite end of each cable. Each stud ring was then placed under a 1.6 cm by 1.1 cm conductive fabric patch (EeonTex conductive fabric) to create an electrode. The conductive fabric patches were adhered with glue at the edges to non-conductive fabric acting as the belt. By custom making the belt, the length could be chosen to approximate the girth of the animal models. Thus, ensuring suitable tension of the belt and good electrode contact.

Using this EIT system, the data were collected at a rate of 32 frame/s, with an injection frequency of 97 kHz, an injection current of 2.8 mA_{rms} and a 'skip of' 3 (the electrode gap between the two electrodes used for injection and, equally, between the two electrodes used for measurement).

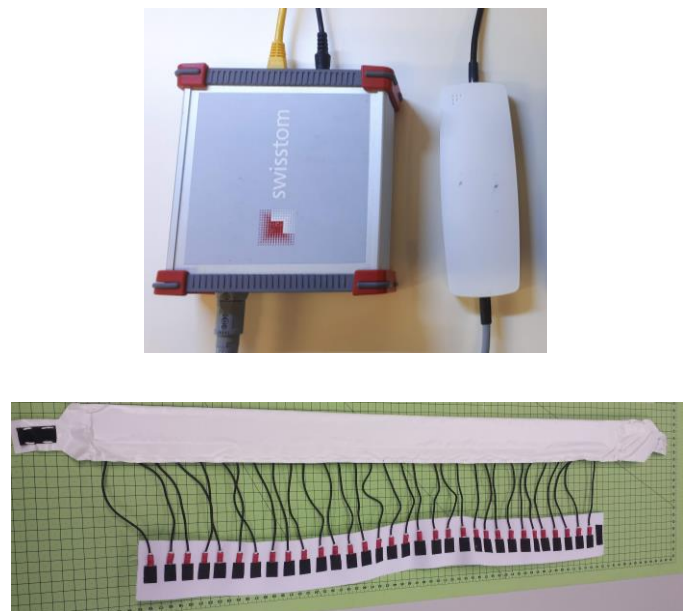


Fig. 2. (top) Swisstom Pioneer Set including the interface module and the sensor belt connector. (bottom) 32 fabric electrode belt. Each black patch is a conductive fabric electrode adhered to the white non-conductive belt fabric.

C. The Animal Model

In this study, VUR was induced in 4 healthy female Danish Landrace/Yorkshire pigs (of mass 31.03 ± 0.39 kg and girth 71.5 ± 0.87 cm). Pigs are commonly employed experimental models in VUR and urological studies [15], [16] as the urinary bladder and the kidneys are similar to those of humans [15]. Human children aged 3-5 years and 18 kg pigs have a similar distance between the renal pelvis of the kidney and the surface of the skin, at approximately 4 cm [17]. However, the pigs

used in our investigation all weighed more than 18 kg (with average weight of 31.03 kg). Therefore, the increased body size represents a more challenging imaging scenario than may be expected with children, as the kidneys are deeper from the surface of the skin in the test animals than they would be in a human child. Importantly, the dielectric properties of tissues for pigs are also similar to those of human tissues [18], [19], ensuring the electrical data gathered from the models in the study represents that of humans as accurately as possible.

D. Experimental Procedure

The experimental setup involved the animal under test being secured and sedated in a supine resting position. Then to mimic VUR, saline solution was infused into one kidney at a time. The saline solution was infused from a gravity fed syringe with a stopcock (Fig. 3) through the ureter to the kidney. The ureters were divided proximal to the urinary bladder by a physician.

The thirty-two fabric electrodes were placed on the skin of the animal under test. The electrodes were spaced equidistantly around the pig and the belt was centered over the kidneys along the longitudinal axis. These electrodes were then connected to the EIT device.

In order to ensure that the electrodes were correctly positioned, a pre-experiment procedure was performed using contrast agent and fluoroscopy imaging. The syringe and stopcock were connected to the ureters using 8 Fr feeding tubes in order to deliver the solution to the kidneys. The syringe was placed at a fixed height (on average 40.75 ± 3.5 cm) above the kidneys to provide a non-damaging flow rate and pressure to the renal pelvis of the kidney [20]. The syringe was filled with 10 ml of 3:1 saline (343 mmol/L Sodium concentration) and contrast agent (Omnipaque, GE Healthcare) solution. The contrast agent was required for the fluoroscopy imaging. Before infusion, the solution was heated in a water bath to match the body temperature of the animal, approximately 39°C . The solution was infused into the ureters and the kidneys in order to visualize the renal system with fluoroscopy and to correctly align the EIT electrodes. The solution was then allowed to drain out of the kidneys for two minutes by temporarily disconnecting the syringe from the feeding tube.

Once the electrodes were correctly placed, the syringe was filled with 10 ml of saline (260 mmol/L Sodium concentration) at 39°C and infused into one kidney at a time. The 10 ml volume was chosen based on the fact that the median urine reflux volume is between 10% and 15% of bladder capacity [21]. The bladder capacity for a child, BC , was estimated by the equation [22] :

$$BC = (Age \text{ in years} + 2) \times 30 \text{ ml.} \quad (1)$$

Thus, the 10 ml volume mimics a difficult VUR detection case in a young child. In addition, in these large porcine models (31.03 ± 0.39 kg), the kidneys are deeper within the body than they would be within a child. The concentration of saline in the solution is designed to mimic a urine conductivity of around 2 S/m. The 2 S/m conductivity is within the urine

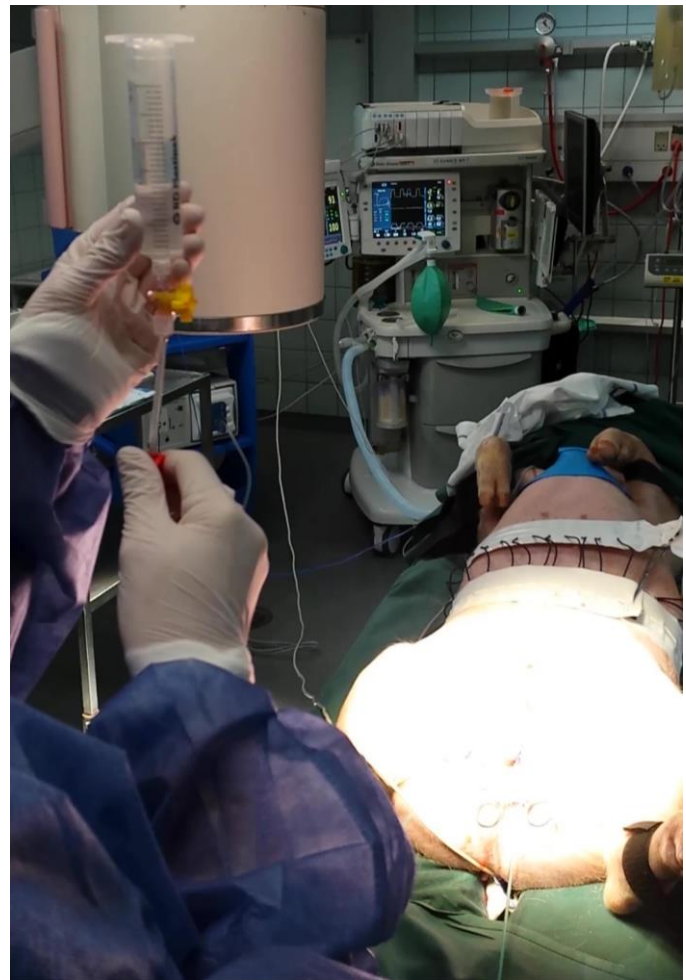
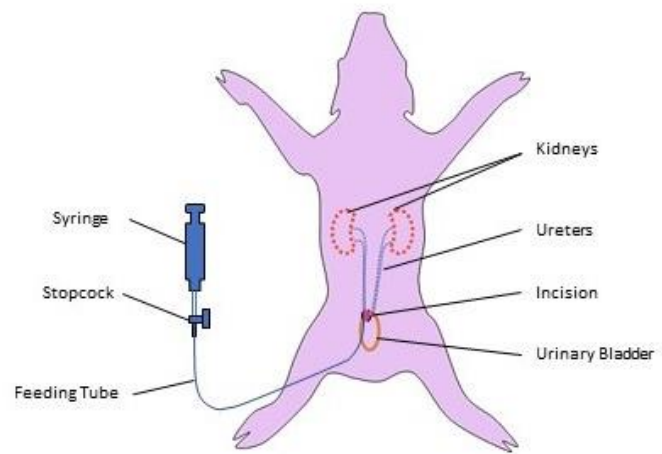


Fig. 3. (top) Illustration of the experimental setup with a supine animal. The solution is infused with a gravity feed once the stopcock is opened. For each experiment, only one kidney is infused, allowing a comparison between the measured conductivities of the two kidneys. (bottom) Experimental setup with one of the porcine models.

conductivity range of 0.5-3.25 S/m of the current literature [23], [24].

The EIT device was used to capture voltage data between all electrode pairs both before and after the infusion. The recording started 20-30 seconds before infusion and was stopped after about 20-30 seconds after infusion started (total

time: 40-60 seconds). The solution was then allowed to drain out of the kidneys, as before, at the end of each experiment.

The infusion of saline was repeated several times for each kidney of each of the four pigs. Specifically, 20 experiments were performed with the first animal model, 30 for each of the second and third pigs, and 36 with the final pig. In each case, half of the total number of experiments involved injection of the left kidney, and half involved injection of the right kidney. In total, 116 experiments were performed.

During the experiment, both the heart rate and the temperature of the pig were monitored to detect any irregularities.

To control breathing artefacts, the pigs were attached to a mechanical ventilator that controlled the breathing rate. The breathing rate applied was controlled between 5-15 breaths per minute.

III. IMAGE RECONSTRUCTION & ANALYSIS

A. Data Preprocessing

To remove high-frequency noise that could potentially affect the quality of the raw voltage data and the reconstructed images, a 10th order Butterworth low pass filter was applied to the voltage frames. The cutoff frequency was determined from spectral analysis and set to 0.5 Hz. The measurements from the injection and nearest neighbor's electrodes in EIT have been shown to decrease the performance of the resultant images [25]. Thus, we removed the measurements from the injection and the two nearest electrodes in order to produce higher quality images. This preprocessing step resulted in 19 measurements per injection pair, with 608 total voltage measurements per frame (i.e., 19 measurements x 32 injection pairs = 608 total measurements).

B. Image Reconstruction

For image reconstruction, an elliptical cylindrical finite element model (FEM) representing the abdomen boundary of the animal model was used as the forward model. The FEM also contained 32 equidistance electrodes around the boundary. The Graz consensus Reconstruction algorithm for EIT (GREIT) [26] was used as the time-difference image reconstruction algorithm. The reference data for each experiment were taken as the frames captured the five seconds immediately before the infusion. Images of size 64x64 pixels were produced using the GREIT optimization parameters of the noise figure of 0.5 and a target radius of 0.2. These parameters are discussed by Adler et al. in [26].

C. Image Analysis

Based on knowledge of where the kidneys were located from fluoroscopy images, two regions of interest (ROIs) corresponding to each kidney location were identified. The pixel intensity correlating to the conductivity change within each region was then analyzed. Each ROI had a radius of five pixels to fully capture the target areas, as EIT suffers from low transitions [27]. For further analysis, we also extracted the mean pixel intensity curves from the ROIs. The effects of breathing were removed from the mean pixel intensity curves by smoothing with a weighted linear least squares local regression and a 2nd degree polynomial model.

IV. CRITERIA FOR DETECTION

In order to objectively determine that the difficult but realistic scenario of a 10 ml volume in the porcine model was detected at the kidneys, we performed statistical analysis on both pre-processed voltage data and on the images from each experiment.

First, for each experiment, we gather an equal number of frames before and 10 seconds after the start of infusion in order to compare fairly using statistical analysis. A 10 seconds transition interval was chosen as this allowed sufficient time for the majority of the infusion to have occurred and to be identified in the signals, as can be seen in Fig. 4. This data was used then for comparing the before and after infusion in both voltage and images. The time interval for recorded data (the sample size) before and 10 seconds after the start of infusion was fixed at around 15 seconds (i.e., 452.78 ± 53.32 frames), varying slightly based on the recording length. Analyzing a longer duration of data before and after infusion reduces the impact of random experimental noise. However, a shorter duration can also be considered if necessary, since EIT can record tens of frames per second, and changes are seen in Figs. 4 and 7 to occur within a few seconds.

A t-test was used to compare the mean of the voltage frames collected before infusion to the mean of those frames collected 10 seconds after the start of the infusion. As the conductivity of the body increases, the voltage is driven down by the current controlled EIT system. Thus, we expect the mean voltage before infusion to be larger than the mean voltage after infusion. We used a two-sample student t-test with an alpha level of 0.01 and given samples of equal size to determine if there was a statistically significant difference in the voltage signals before and 10 seconds after the start of infusion. The t-test is left-sided as we expect the voltages 10 seconds after the start of infusion to be significantly less than the voltages before infusion.

Next, we examine the reconstructed time-difference images. Two comparisons are analyzed: i) the images of one kidney, before and 10 seconds after the start of the infusion, and ii) the images of the infused kidney versus non-infused kidney. We do the two comparisons for images instead of just i), like in the voltage data comparison, as with images we have the benefit of spatial information to determine the exact data from the target regions. Therefore, doing comparison ii) in voltage data is not straightforward. In both cases, i) and ii), the mean of the pixel intensities within the ROI was compared. For the kidney to be infused, the conductivity of the ROI should increase with infusion; while the ROIs of the kidney before infusion and of the not-infused kidney should have a relatively constant conductivity over time. Thus, for both image comparisons, we performed a right-sided two-sample student t-test with an alpha level of 0.01 using the mean pixel intensities from the ROIs.

If a significant change is found in voltage data and reconstructed images between non-infused and infused measurements, then we can confidently and objectively detect VUR.

V. RESULTS AND DISCUSSION

In this section, we analyze the results from the objective detection test, and the differences between the infused kidney and the normal, not infused kidney, across all experiments.

A. Experimental Factors

The average injection volume was 9.56 ± 0.69 ml. A precise injection of 10 ml was not possible as in some of the experiments the infusion stopped when the renal pelvic region of the kidney was full for the given pressure. Smaller infusions were deemed appropriate as they represent a worst-case scenario. No temperature or heart rate readings went outside the normal range during the study i.e., no irregularities were observed. The mean contact impedance of the electrodes on the skin was sufficiently low at $318.13 \pm 29.62 \Omega$.

B. Raw Voltage Analysis

Using the detection tests outlined in Section IV, the infused volume was detected in 94.83% of the experiments using the collected voltage data. The six experiments (out of 116) where VUR was not detected with the voltage data, were due to increased noise attributed to experimental error, insufficient draining from the previous experiment, and high pressure in the kidney.

An example of a detected voltage signal is given in Fig. 4. The signal contains the artificially controlled breathing. The mean voltage signal drops in amplitude during and after infusion and remains at a lower voltage level than before infusion.

Further investigating all the experiments, Fig. 5 shows the mean voltage difference between before and after infusion for the experiments in each pig. The majority of experiments show a lower mean voltage for the measurements after infusion than those before infusion. However, the overall difference is much less for Pigs 3 and 4 than for Pigs 1 and 2. Some experiments in Pig 3 and 4 even show a greater mean voltage during infusion than after. From analyzing the detection results, three of the six misclassified experiments based on voltage data were from Pig 3 while the other three came from Pig 4, which makes sense based on the data of Fig. 5.

The mean voltage can be easily affected by outlier voltages within the frame such as those affected by noise. However, by analyzing the measurements from electrodes nearer to the kidney, we found the expected trend even for the six previously misclassified voltages cases. This finding suggests that selection of specific injection-measurement voltages, or optimization of electrodes positions, may further increase the detection abilities of the system.

While detection of VUR using the voltage data shows promise, image-based detection may provide enhanced detection capabilities due to the addition of spatial information.

C. Objective Image Analysis

The small infused volume was detected with a 99% confidence interval in 98.28% of experiments when comparing the infused ROI of the images before and 10 seconds after the start of infusion and in 100% of

experiments when comparing infused versus non-infused ROIs in the reconstructed images.

Overall, by transforming the voltage data into spatial information using image reconstruction, the kidney reflux is more accurately detected than with the processed voltage signals. The reconstructed images, as shown in Fig. 6, are also more easily interpreted than the voltages. Using the images, we can also observe how the mean pixel intensity in the ROIs change during the infusion by looking at the pixel intensity-time graph, as shown in Fig. 7. We can see that the mean pixel intensity over the course of an infusion increases in the infused right kidney and remains near constant for the non-infused left kidney. The trends presented in Figs. 6 and 7 are

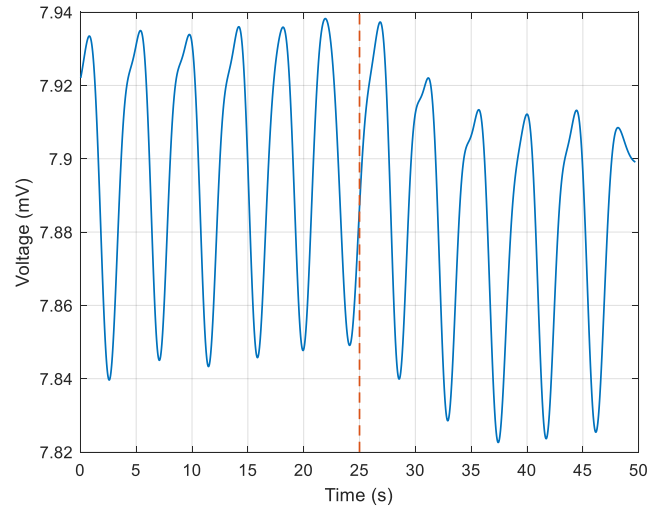


Fig. 4. An example of a detected VUR occurrence in the voltage signals. The voltage drops on infusion (the start of infusion is at 25 seconds, which is marked by the orange dotted line) and the new voltage level remains lower than the voltage level before infusion.

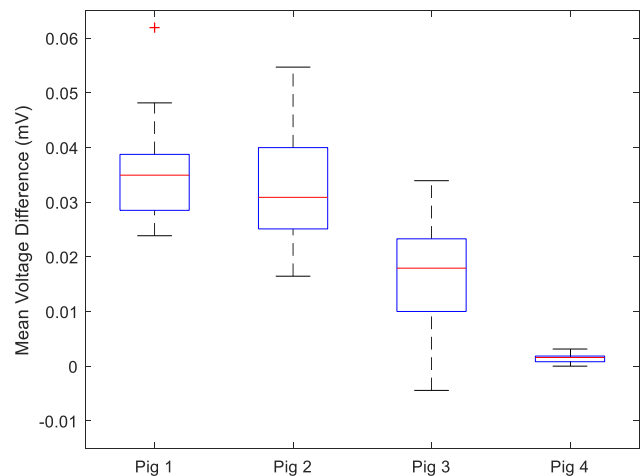


Fig. 5. Mean voltage difference between before and during infusion for the experiments performed in each pig. The boxplot indicates the overall median with the horizontal red line, the 25th and 75th percentiles with the box edges, and the extreme points with the whiskers (not including the outliers, which are marked by a plus symbol). Overall, the mean voltage difference is strong between before and during infusion (0.02 mV), particularly for Pig 1 and 2. However, the mean voltage difference is lower for Pigs 3 and 4. For Pig 3, some values are negative, indicating that the mean infusion voltage was greater than before infusion. However, overall the mean for Pig 3 is greater than 0.01 mV.

similar across all of the EIT experiments for each injected kidney and animal.

For all experiments, Fig. 8 shows the difference in mean pixel intensity between before and 10 seconds after the start of the infusion. In this case, the comparison considers only the ROI of the kidney that is being infused. The mean pixel intensity difference varies across all experiments between 0.004 to 0.32, with a mean of 0.21. Similarly, Fig. 9 shows the difference in mean pixel intensity between the infused and non-infused kidneys (i.e., comparing the controlled kidney and the infused kidney). In this case, the mean pixel intensity

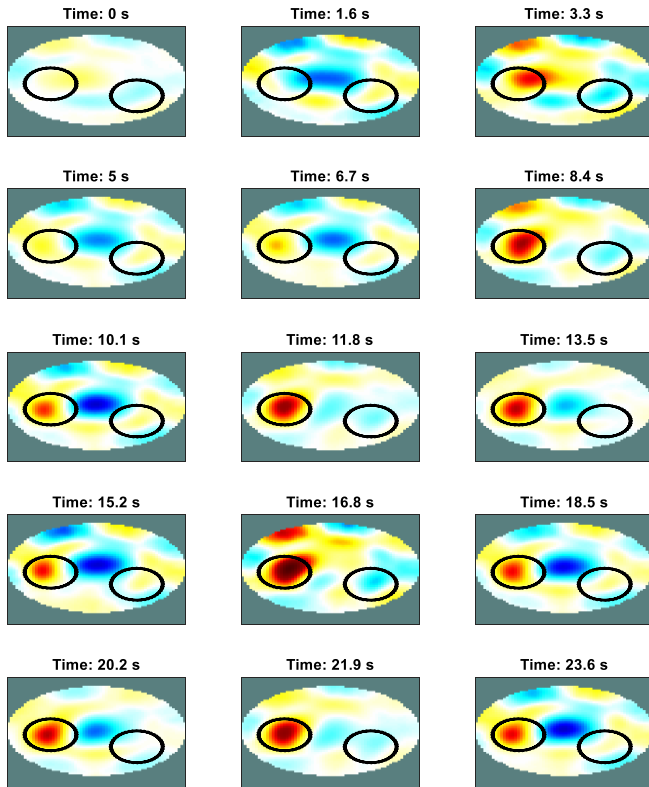


Fig. 6. Series of EIT images reconstructed from the start of infusion to near the end. The ROIs are given by the black circles in each image. Deep red represents the highest conductivity, while blue represents the low conductivity. The gray border in each image delimits the region outside the FEM. During this experiment, the right kidney was infused with the saline solution (left ROI). This infusion can be clearly seen in the reconstructed EIT images. In the images corresponding to 5 s and 6.7 s, reduced intensity of the infused region was caused by breathing artefacts. Further, breathing artefacts also appear in the images with a blue circle centered in a number of images (e.g. at time 23.6 s) that is consistent with peak exhalation in the data.

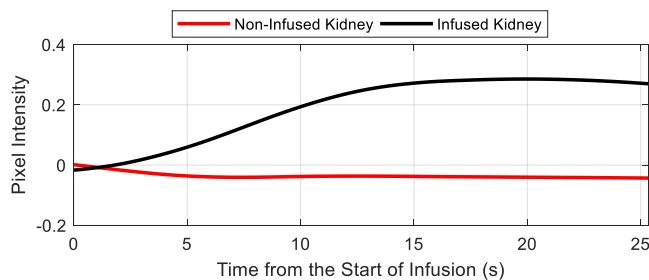


Fig. 7. Pixel intensity curves from the ROIs shown in Fig. 6. As the infusion progresses, the conductivity in the infused kidney increases, while the conductivity of the non-infused kidney remains approximately constant. Breathing artefacts were removed using smoothing, as outlined in Section III.

difference between the infused and non-infused images is 0.11 and 0.41 with a mean of 0.26.

As seen in Figs. 8 and 9, the spatial information for Fig 4 seems to overcome the poor change in the mean voltage in Fig. 5. As discussed in Section V.B, the mean voltage can be easily affected by outlier voltages within the frame such as those affected by noise and voltages that may not be from the ROI. However, selection of specific injection-measurement voltages, or optimization of electrodes positions, may further increase the detection abilities of the system.

Overall, there is a strong difference between infused and non-infused regions, as is clear from Figs. 8 and 9. These figures also explain the high 98.28% and 100% detection rates seen with the image data, since the mean pixel intensity differences are generally large.

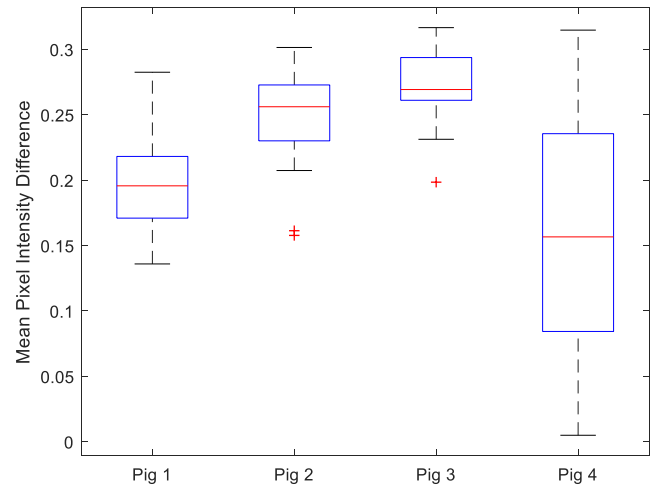


Fig. 8. Mean pixel intensity difference of before and 10 seconds after the start of infusion for the infused kidney in each of the experiments performed in the four pigs. Overall, there is a strong difference between before and 10 seconds after the start of infusion, particularly for Pigs 2 and 3.

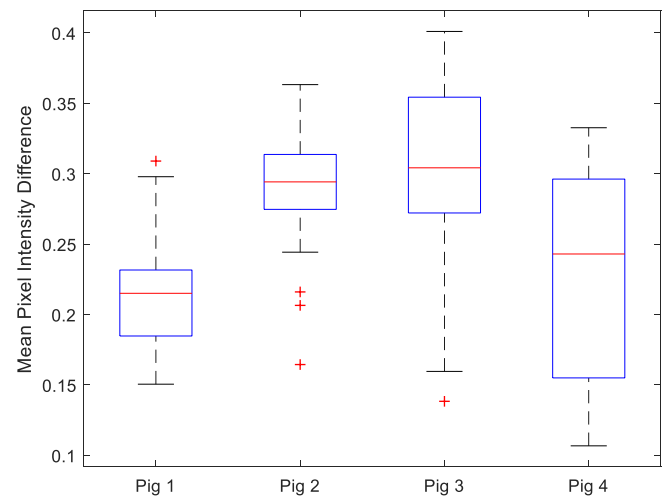


Fig. 9. Mean pixel intensity difference between the infused and non-infused kidneys for the experiments performed in each pig. Overall, there is a strong difference between the infused and non-infused kidney, particularly for Pigs 2 and 3.

D. Study Limitations

In this study, we controlled factors such as breathing and movement by mechanical-ventilation and by anesthetizing the animal models. By controlling these factors, we were able to provide a proof-of-concept for EIT-based VUR detection in a near-ideal clinical case.

However, for the target application of screening VUR in children in clinical scenarios, applying these controls may not be feasible. As such, these factors may need to be handled by employing appropriate signal-processing techniques to filter the signals. This topic is an avenue of future research.

Additionally, the position of the electrodes in this study were confirmed using fluoroscopy. In the clinical scenario, this would not be desirable. However, the location of the kidneys may be determined by physician experience or by using ultrasound. Further, a 3D electrode array (as opposed to a single ring), may be considered to fully cover the region of interest and to increase resolution. Such an array would also reduce the need for precise positioning.

Lastly, in this study, we controlled the infusion time at approximately 20 seconds. In VUR, the reflux would be observable at the time of, and during, voiding. The controlled time allowed us to be consistent across all animals as in bladder capacity and voiding times vary inter-individual [28]. Despite this limitation in terms of the realistic-ness of the timing of VUR, it must be noted that the timing does not affect the detection capability. EIT has high temporal resolution, and this study demonstrates that changes in the kidneys due to reflux can be detected by either comparing before/after the reflux occurs, or by comparing the left/right sides.

Future work will include refinement of the EIT system and the associated signal processing and detection algorithms in order to address these limitations.

VI. CONCLUSION

In this paper, we presented, to our knowledge, the first study examining the use of EIT to detect VUR i.e., the backflow of urine into the kidney, in an animal model. We infused urine-mimicking solution into the ureters of sedated porcine models in order to mimic reflux. EIT data from around the kidneys was collected before, during, and after each infusion. The voltage data were preprocessed, and then time-difference images were reconstructed to examine the reflux over time. We found unilateral VUR was detected in over 98.28% of the reconstructed images and 94.83% in the mean voltage data. The reduced detection in the voltage data came from experimental noise. However, by analyzing the electrodes near where the infusion occurred, the expected trend was observed. Overall, statistically significant differences were found before and after infusion across all 116 experiments. The resultant images are of high quality, showing the infused region with significant clarity. Curves relating to the conductivity can be extracted from images for each kidney, which also show the change during the infusion.

Limitations of this study include controlled breathing and movement of the animal models, which may not be representative of a clinical situation. However, future work will involve refinement of the proposed EIT system and testing the designed system in pilot studies on humans.

This study has successfully demonstrated detection of VUR on animals at the kidneys using the technology of EIT. The results show promise for using EIT for screening VUR in children non-invasively and safely.

ACKNOWLEDGEMENT

The authors would like to thank Ricardo Eleuterio for his significant contribution to this research while at the National University of Ireland, Galway. The authors would also like to thank Aarhus University, Denmark, for their support in conducting the experiments.

REFERENCES

- [1] M. A. Sargent "What is the normal prevalence of vesicoureteral reflux?," *Pediatr Radiol.* vol. 30, no. 9, pp. 587-593, 2000.
- [2] P. Puri, M. Hunziker, "Vesicoureteral Reflux," in *Newborn Surgery*, 4th ed. New York: CRC Press, 2018, pp. 1079-1087.
- [3] P. Puri et al., "Genetics of Vesicoureteral reflux" *Nat Rev Urol.*, vol. 8, no. 10, pp. 539-552, 2011.
- [4] R. L. Lebowitz, et al., "International system of radiographic grading of vesicoureteric reflux," *Pediatr. Radiol.*, vol. 15, no. 2, pp. 105-109, 1985.
- [5] D. H. Chand et al., "Incidence and severity of vesicoureteral reflux in children related to age, gender, race and diagnosis," *J Urol.*, vol. 170, no. 4.2, pp. 1548-1550, 2003.
- [6] N. Shaikh et al., "Dimercaptosuccinic acid scan or ultrasound in screening for vesicoureteral reflux among children with urinary tract infections," *Cochrane Database Syst. Rev.*, no. 7, pp. 1-123, 2016.
- [7] P. Puri, "Endoscopic treatment of vesicoureteral reflux," in *Pediatric Surgery*. Berlin, Germany: Springer, pp. 491-498, 2006.
- [8] C. P. Nelson et al. "Ultrasound as a screening test for genitourinary anomalies in children with UTI," *Pediatrics*, vol. 133, no. 3, pp. 394-403, 2014.
- [9] A. J. Schaeffer et al., "Variation in the level of detail in pediatric voiding cystourethrogram reports," *J. Pediatr. Urol.*, vol. 13, no. 3, pp. 257-62, 2017.
- [10] G. Marra et al., "Congenital renal damage associated with primary vesicoureteral reflux detected prenatally in male infants," *J. Pediatr.*, vol. 124, no. 5.1, pp. 726-30, 1994.
- [11] T. K. Mattoo, "Vesicoureteral reflux and reflux nephropathy," *Adv. Chronic Kidney Dis.* vol. 18, no. 5, pp. 348-54, 2011.
- [12] A. J. Hamilton et al. (2016), UK Renal Registry 18th Annual Report: Chapter 4 Demography of Patients Receiving Renal Replacement Therapy in Paediatric Centres in the UK in 2014. *Nephron.* vol. 132, Suppl 1, pp. 99-110.
- [13] I. Frerichs et al., "Chest electrical impedance tomography examination, data analysis, terminology, clinical use and recommendations: consensus statement of the TRanslational EIT developmeNt stuDy group.," *Thorax*, p. thoraxjnl-2016-208357, 2016.
- [14] E. Dunne et al., "Supervised Learning Classifiers for Electrical Impedance-based Bladder State Detection," *Sci. Rep.*, vol. 8, no. 1, p. 5363, 2018.
- [15] A. Atala et al., "Endoscopic Treatment of Vesicoureteral Reflux with a Self-Detachable Balloon System," *J. Urol.*, vol. 148, no. 2, pp. 724-727, 1992.
- [16] H. J. S. Bagetti Filho, et al., "Pig Kidney: Anatomical Relationships Between the Renal Venous Arrangement and the Kidney Collecting System," *J. Urol.*, vol. 179, no. 4, pp. 1627-1630, 2008.
- [17] B. W. Snow and M. B. Taylor, "Non-invasive vesicoureteral reflux imaging," *J. Pediatr. Urol.*, vol. 6, no. 6, pp. 543-549, 2010.
- [18] A. Peyman and C. Gabriel, "Cole-Cole parameters for the dielectric properties of porcine tissues as a function of age at microwave frequencies," *Phys. Med. Biol.*, vol. 55, no. 15, pp. N413-N419, 2010.
- [19] C. Gabriel, "Compilation of the Dielectric Properties of Body Tissues At RF and Microwave Frequencies," Brooks AFB, San Antonio, TX, Contract AL/OE-TR-1996-0037, 1996.
- [20] D. J. Griffiths et al., "Dynamics of the upper urinary tract: II. The effect of variations of peristaltic frequency and bladder pressure on pyeloureteral pressure/flow relations," *Phys. Med. Biol.*, vol. 32, no. 7, pp. 823-833, 1987.

- [21] S. Sjöström et al., "Change of Urodynamic Patterns in Infants With Dilating Vesicoureteral Reflux: 3-Year Followup," *J. Urol.*, vol. 182, no. 5, pp. 2446–2454, 2009.
- [22] S. Koff, "Estimating bladder capacity in children.," *Urology*, vol. 21, no. 3, p. 248, 1983.
- [23] T. Schlebusch et al., "Impedance ratio method for urine conductivity-invariant estimation of bladder volume," *J. Electr. Bioimpedance*, vol. 5, no. 1, pp. 48–54, 2014.
- [24] E. Dunne et al., "A realistic pelvic phantom for electrical impedance measurement," *Physiol. Meas.*, vol. 39, no. 3, p. 034001, 2018.
- [25] V. Kolehmainen et al., "Assessment of errors in static electrical impedance tomography with adjacent and trigonometric current patterns," *Physiol. Meas.*, vol. 18, no. 4, pp. 289–303, 1997.
- [26] A. Adler et al., "GREIT: a unified approach to 2D linear EIT reconstruction of lung images," *Physiol. Meas.*, vol. 30, no. 6, pp. S35–S55, 2009.
- [27] E. Dunne, et al., "Image-based classification of bladder state using electrical impedance tomography," *Physiol. Meas.*, vol. 39, no. 12, p. 124001, 2018.
- [28] N. Hirahara et al., "Four-dimensional ultrasonography for dynamic bladder shape visualization and analysis during voiding.," *J. Ultrasound Med.*, vol. 25, no. 3, pp. 307–13, 2006.